JACS
JOURNAL OF THE AMERICAN CHEMICAL SOCIETY
Article
pubs.acs.org/JACS

Ionic and Neutral Mechanisms for C–H Bond Silylation of Aromatic Heterocycles Catalyzed by Potassium *tert*-Butoxide

Shibdas Banerjee,[†,#] Yun-Fang Yang,[‡,#] Ian D. Jenkins,[∥,#] Yong Liang,[‡] Anton A. Toutov,[§] Wen-Bo Liu,[§] David P. Schuman,[§] Robert H. Grubbs,[§] Brian M. Stoltz,[§] Elizabeth H. Krenske,*[,⊥] Kendall N. Houk,*[,‡] and Richard N. Zare*[,†]

[†]Department of Chemistry, Stanford University, Stanford, California 94305-5080, United States
[‡]Department of Chemistry and Biochemistry, University of California, Los Angeles, California 90095-1569, United States
[∥]Eskitis Institute, Griffith University, Nathan, QLD 4111, Australia
[⊥]School of Chemistry and Molecular Biosciences, The University of Queensland, Brisbane, QLD 4072, Australia
[§]Division of Chemistry and Chemical Engineering, California Institute of Technology, Pasadena, California 91125, United States

Supporting Information

ABSTRACT: Exploiting C–H bond activation is difficult, although some success has been achieved using precious metal catalysts. Recently, it was reported that C–H bonds in aromatic heterocycles were converted to C–Si bonds by reaction with hydrosilanes under the catalytic action of potassium *tert*-butoxide alone. The use of Earth-abundant potassium cation as a catalyst for C–H bond functionalization seems to be without precedent, and no mechanism for the process was established. Using ambient ionization mass spectrometry, we are able to identify crucial ionic intermediates present during the C–H silylation reaction. We propose a plausible catalytic cycle, which involves a pentacoordinate silicon intermediate consisting of silane reagent, substrate, and the *tert*-butoxide catalyst. Heterolysis of the Si–H bond, deprotonation of the heteroarene, addition of the heteroarene carbanion to the silyl ether, and dissociation of *tert*-butoxide from silicon lead to the silylated heteroarene product. The steps of the silylation mechanism may follow either an ionic route involving K^+ and $^tBuO^-$ ions or a neutral heterolytic route involving the $[KO^tBu]_4$ tetramer. Both mechanisms are consistent with the ionic intermediates detected experimentally. We also present reasons why KO^tBu is an active catalyst whereas sodium *tert*-butoxide and lithium *tert*-butoxide are not, and we explain the relative reactivities of different (hetero)arenes in the silylation reaction. The unique role of KO^tBu is traced, in part, to the stabilization of crucial intermediates through cation–π interactions.

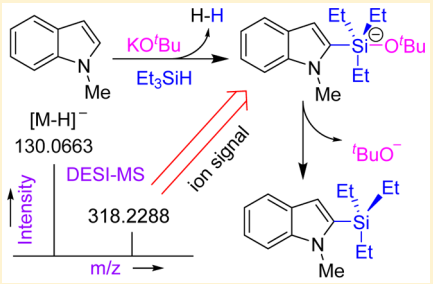

INTRODUCTION

More than 90% of industrial chemical processes employ catalysis.[1] Most catalysts rely upon metals, often transition metals that are very expensive and may require supporting ligands, and the overall processes are not environmentally benign. Therefore, sustainable development of transition-metal-free catalysis is highly important.[2] A number of literature precedents have substantiated the usefulness of potassium *tert*-butoxide (KO^tBu) as a catalyst for different types of coupling reactions.[2−8] Recently, Toutov et al.[9] reported the direct silylation of C–H bonds in aromatic heterocycles, with excellent regioselectivity and good yield, by using KO^tBu as the catalyst and hydrosilanes as a convenient and inexpensive silicon source, as shown in Scheme 1. Although the initial study did not lead to a conclusive understanding of the reaction mechanism, a combined experimental and theoretical effort has helped us to conceive of two independent mechanisms (radical and ionic) that may drive the silylation reaction. It is not surprising that a reaction may have more than one mechanism.[10−12] The accompanying paper,[13] communicated together with this manuscript, describes the radical mechanism for this reaction. We present here the ionic mechanism of the KO^tBu catalyzed silylation of heteroaromatic C–H bonds.[9] Evidence from ambient ionization mass spectrometry (MS), conductivity measurements, and density functional theory (DFT) calculations identifies the ionic species (intermediates) present in the reaction mixture and leads to the proposal of two heterolytic mechanisms that are consistent with all reaction

Scheme 1. KO^tBu-Catalyzed Silylation of Indoles

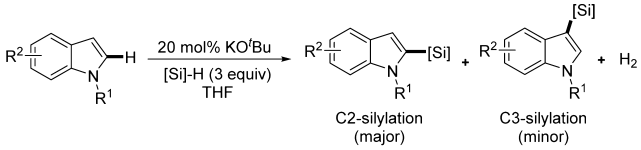

R^1 = -Me, -Et, -Ph, $-CH_2Ph$, $-CH_2OMe$ or $-CH_2O(CH_2)_2SiMe_3$
R^2 = -H, -Me, -Ph, -OMe, $-OCH_2Ph$ or $-CH_2OMe$
[Si]-H = Et_3SiH, Et_2SiH_2, $EtMe_2SiH$, $PhMe_2SiH$ or $^nBu_3SiH$

Received: December 19, 2016
Published: May 2, 2017

DOI: 10.1021/jacs.6b13032
J. Am. Chem. Soc. XXXX, XXX, XXX−XXX

features previously observed by Toutov et al.[9] as well as explaining possibly the sudden onset of the reaction (vide infra).

RESULTS AND DISCUSSION

Detection of Ionic Intermediates by DESI-MS. To detect the transient ionic intermediate(s) in the solution-phase reaction, we employed desorption electrospray ionization mass spectrometry (DESI-MS; see Supporting Information (SI), Supplementary Note 1).[14] The details of the DESI-MS experimental setup are shown in Figure S1 of the SI. During the course of the KO^{t}Bu-catalyzed reaction of 1-methylindole (MI) with triethylsilane (Et_3SiH) in tetrahydrofuran (THF) (Scheme 1, where R^1 = Me, R^2 = H, and [Si]-H = Et_3SiH; see Experimental Section for details), we detected the formation of deprotonated MI (m/z 130.0663; Figure 1a) by DESI-MS. The

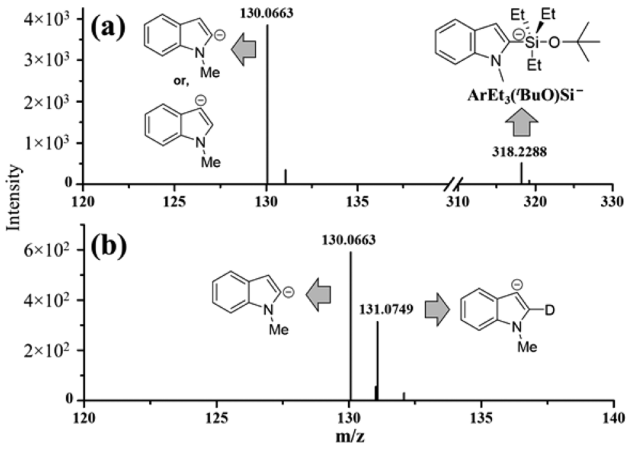

Figure 1. Negative ion mode DESI mass spectra (background subtracted) for the silylation reaction of (a) 1-methylindole and (b) C2-deuterated (~95% labeled) 1-methylindole.

same ion (m/z 130.0663) was not detected in control experiments where pure MI or a mixture of MI and Et_3SiH were analyzed (data not shown). Protons C2 and C3 in the pyrrole ring of 1-methylindole are comparatively acidic in nature.[15] As the C2 proton is more acidic than the C3 proton (C2 proton pK_a ≈ 37 and C3 proton pK_a ≈ 42 in THF),[15] the C2 proton is expected to be preferentially abstracted by a strong base, present in the reaction medium. To verify this, we performed the corresponding reaction on C2-deuterated MI (Figure 1b). Although the bond strength of C2−D is slightly higher than that of C2−H, we were still able to detect the deuterium-abstracted species (m/z 130.0663) as a major anion and the proton-abstracted species (m/z 131.0749) as a minor anion from C2-deuterated MI substrate. These results, in conjunction with the reported regioselectivity (C2-[Si]:C3-[Si] > 20:1),[9] clearly suggest that a proton from the pyrrole ring of MI is abstracted during the reaction, and that the C2 proton is preferentially abstracted relative to the C3 proton.

Along with deprotonated MI, an ion signal at m/z 318.2288 corresponding to the pentacoordinate silicon species $ArEt_3(^tBuO)Si^-$ was also detected in the reaction mixture (Figure 1a). Presumably, this hypervalent silicon intermediate proceeds to form the product in the catalytic cycle. We also detected the K^+ complex of the product (silylated MI) by DESI-MS under positive ion mode (SI, Figure S2), indicating a cation−π interaction involving K^+ and the "π-excessive" indole moiety.[16] In a separate DESI-MS control study, we mixed pure C2-silylated product (R^1 = Me, R^2 = H, [Si] = $SiEt_3$ in Scheme 1) and KO^{t}Bu, but we did not detect the $ArEt_3(^tBuO)Si^-$ (m/z 318.2288). This result suggests that this species is predominantly formed during the course of the reaction (Figure 1a), not by the interaction of the product and *tert*-butoxide ion.

Likewise, a DESI-MS study of the silylation reaction of another type of substrate, i.e., dibenzofuran,[9] intercepted deprotonated dibenzofuran species from the reaction mixture (SI, Figure S3).

We also performed a time-dependent study on detecting the above anionic intermediates using DESI-MS after starting the reaction. The intermediates were detected only after 1 h of the reaction time, indicating that (1) the reaction occurred in the bulk phase, not in DESI microdroplets,[17,18] and (2) there is an induction period for the reaction to occur. The intermediates were transferred to gas phase from the condensed phase (reaction mixture) by the DESI soft ionization process.

An Ionic Mechanism. On the basis of the above observations, and considering all of the other reaction features originally reported by Toutov et al.,[9] Scheme 2 presents a

Scheme 2. Proposed Ionic Mechanism for the Catalytic Cycle of the Silylation Reaction

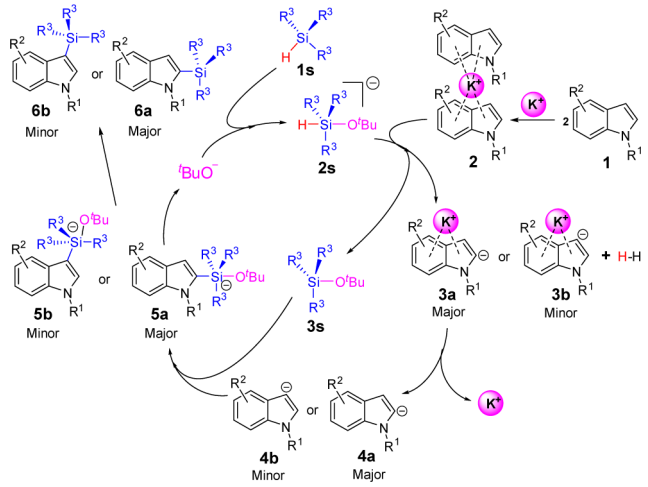

plausible ionic mechanism for the silylation reaction. In the first step of the mechanism, the "π-rich" heteroarene (**1**) interacts with K^+ to form a cation−π complex **2** (detected, see later). Complexation makes the heteroarene protons C2−H and C3−H more acidic, facilitating deprotonation by a strong base. Although the most obvious base present in the reaction mixture is $^tBuO^-$, we propose that $^tBuO^-$ does not directly deprotonate **2** but instead reacts with the silane **1s** to form a pentacoordinate silicon complex (**2s**) (see SI, Supplementary Note 2) and that **2s** becomes a source of hydride ion to abstract the acidic proton from **2**. This proposed step resembles the formation of hydride ions by the reaction between metal alkoxide and hydrosilane reported earlier.[19] However, from the present experimental data we cannot ascertain whether proton abstraction from the heteroarene substrate by the leaving hydride group of **2s** occurs in a concerted or a stepwise way. Deprotonation of **2** leads to the formation of ion pairs **3a** (major) and **3b** (minor), with hydrogen gas as a byproduct (detected, see Figure 3a).

Ion pair **3a**/**3b** is proposed to dissociate to give the anions **4a**/**4b** (deprotonated heteroarene) that were unambiguously

DOI: 10.1021/jacs.6b13032
J. Am. Chem. Soc. XXXX, XXX, XXX−XXX

detected in the DESI-MS experiment (Figure 1). These reactive, nucleophilic heteroarene carbanions **4a**/**4b** are proposed to attack the silyl ether **3s** to form pentacoordinate silicon intermediate **5a**/**5b**, which was also detected by DESI-MS (Figure 1a). Subsequent dissociation of $^{t}BuO^{-}$ from **5a**/**5b** leads to the products **6a**/**6b**, which can form a cation−π complex with K^{+} (SI, Figure S2).

Evidence for Cation−π Complex Formation. As **3a** and **3b** are neutral, MS cannot detect them. However, the precursor cation−π complex **2** was detected by ESI-MS (see below), and the proposed deprotonation of **2** leading to ion pairs **3a** and **3b** is supported by the observation that indole substrates possessing electron-withdrawing groups (-NO_2, -CN, etc.) were unreactive to catalysis.[9] The π-electron deficiency of these heteroarenes would inhibit the formation of cation−π complex **2**. As expected, we did not observe any deprotonated species from these heteroarenes (Ar-NO_2, Ar-CN, etc.) when the corresponding reaction mixtures were studied by DESI-MS.

Further support for the reaction route from **1** to **2** to **3a**/**3b** comes from ESI-MS.[20] When we electrosprayed a methanolic solution of MI containing Li^{+}, Na^{+}, and K^{+} ions in an equimolar ratio, we detected the formation of cation−π complexes (Figure 2). Although we did not detect the ion signal of $[MI+M]^{+}$, we

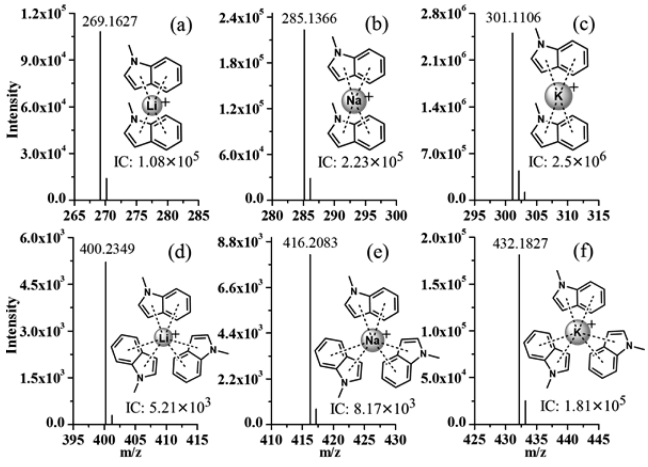

Figure 2. ESI mass spectra indicating the cation−π interactions involving Li^{+}/Na^{+}/K^{+} and 1-methylindole (MI). A methanolic solution of MI containing lithium acetate, sodium acetate, and potassium acetate, each at concentration of 10 mM, was electrosprayed in positive ion mode, and the corresponding mass spectrum showed the ion signals of different cation−π complexes: (a) $[2MI+Li]^{+}$ m/z 269.1627, (b) $[2MI+Na]^{+}$ m/z 285.1366, (c) $[2MI+K]^{+}$ m/z 301.1106, (d) $[3MI+Li]^{+}$ m/z 400.2349, (e) $[3MI+Na]^{+}$ m/z 416.2083, and (f) $[3MI+K]^{+}$ m/z 432.1827. Strengths of these cation−π interactions are also represented by the values of their ion currents (IC).

detected the ion signal of $[2MI+M]^{+}$ corresponding to cation−π sandwich complexes[21] (e.g., **2**) (Figure 2a−c) and the ion signal of $[3MI+M]^{+}$ corresponding to the interaction of the central metal ion with three heteroarene molecules[22] (Figure 2d−f). Interestingly, for both types of complex, the ion signal (ion current: IC) intensities followed the order: K^{+}-complex > Na^{+}-complex > Li^{+}-complex even though the cation−π interaction strengths are expected to follow the reverse order in the gas phase.[22] The trade-off between solvation and cation−π interaction modifies the strength of the cation−π interaction in solution (K^{+}-complex > Na^{+}-complex > Li^{+}-complex)[23] and hence results in the highest signal intensity for the K^{+}-complex and the lowest signal intensity for the Li^{+}-complex. Earlier studies also support the proposal that K^{+} forms stronger cation−π interactions with arenes in solution than does Na^{+} or Li^{+}.[23−25] These findings on the relative strengths of the cation−π interactions suggest one possible explanation for the ineffectiveness of $NaO^{t}Bu$ and $LiO^{t}Bu$ as catalysts for the dehydrogenative C−H silylation.

Nuclear magnetic resonance (NMR) spectroscopy provided further evidence for cation−π complex formation. We recorded the ^{1}H NMR spectra (SI, Figure S4) of methanolic (CD_3OD) solutions of MI containing Li^{+}, Na^{+}, or K^{+}. The chemical shifts of the aromatic protons differed for different salt solutions. Downfield peak shifting was observed, the magnitude of which followed the order: K^{+} solution > Na^{+} solution > Li^{+} solution. This result once again indicates that K^{+} possesses a higher affinity for MI in solution than does Na^{+} or Li^{+}.

When the silylation reaction was attempted using $LiO^{t}Bu$ or $NaO^{t}Bu$ as catalyst, no product was detected, even when the reaction was run for 5 days.[9] We detected no ion signal of deprotonated MI in a DESI-MS experiment when the reaction was run using $LiO^{t}Bu$ or $NaO^{t}Bu$ (SI, Figure S1). The lack of reactivity of $LiO^{t}Bu$ or $NaO^{t}Bu$ might be attributed to the looser cation−π interactions of Li^{+} or Na^{+} with MI, which may limit dissociation of the metal alkoxide and/or activation of the heteroarene. Another relevant observation in the original report was that addition of 18-crown-6 to the reaction mixture decelerated the reaction.[9] Trapping of K^{+} as the 18-crown-6 complex[26] (detected in a DESI-MS experiment; see SI, Figure S5) decreases the availability of the K^{+} ion for pairing with the heteroarene (**1**) to form the intermediate cation−π complex (**2**). All these observations collectively support the important role K^{+} may play in driving the reaction through the formation of intermediates **2** and **3a**/**3b**.

Formation of the Hydride Donor To Deprotonate the Heteroarene. Silicon is less electronegative than hydrogen, and the Si−H bond in **1s** possesses some hydridic character.[27] Upon nucleophilic ($^{t}BuO^{-}$) attack, the Si−H bond in the pentacoordinate silicon intermediate **2s** can serve as a hydride donor (SI, Supplementary Note 2).[28−31] Indeed, cleavage of the Si−H bond in hydrosilanes by strong nucleophiles to form alkylated or arylated silanes with loss of hydride is precedented in the literature.[32,33] Therefore, the silane hydrogen in **2s** is expected to be sufficiently basic to abstract a proton from **2** leading to formation of H_2 (detected, see Figure 3a). This proposition is further supported by an isotope labeling experiment: when we used C2-deuterated MI substrate (**1**) in the silylation reaction, we observed the evolution of HD gas (SI, Figure S6).

When different alkoxide bases were used as catalysts in stoichiometric reactions, the reaction efficiencies followed roughly the basicities (i.e., $KO^{t}Bu$ > KOEt > KOMe).[9] This behavior is consistent with the proposed addition of the alkoxide anion to the silane (**1s**) to form the reactive pentacoordinate silicon intermediate (e.g., **2s**).

Conductivity Studies. $KO^{t}Bu$ in THF is reported to have a neutral tetrameric cubane-like structure.[34] DFT calculations in continuum solvent predict that it requires 36 kcal/mol to dissociate $(KO^{t}Bu)_4$ into ions (SI, Figure S7), although this is likely a high estimate, as specific K^{+}−THF interactions would stabilize the ions. In line with this theoretical result, a conductivity study shows that $KO^{t}Bu$ is indeed a poor electrolyte in THF (Figure 3c). However, unlike $NaO^{t}Bu$,

DOI: 10.1021/jacs.6b13032
J. Am. Chem. Soc. XXXX, XXX, XXX−XXX

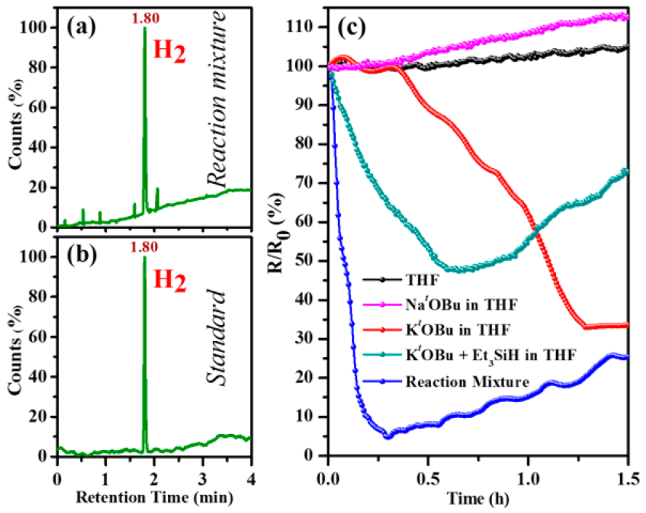

Figure 3. Left panels show the gas chromatographic detection of hydrogen gas from (a) the reaction mixture, and (b) the standard sample. The chromatographic signal intensities (counts) were normalized to 100. The right panel (c) shows the assessment of electrolytic properties of the catalyst, reagents, and the silylation reaction mixture (mixture of MI, KO^{t}Bu, and Et_3SiH in THF) by measuring the resistance (R) over time at 45 °C. R is normalized, showing the relative change of R in percentage over time. See Experimental Section for details.

KO^{t}Bu was found to dissociate gradually to some extent over time until it reached an equilibrium point (~1.3 h in Figure 3c) after which no further dissociation occurred. Conductimetric analysis of a silylation reaction mixture (MI, KO^{t}Bu, Et_3SiH in THF) showed a steep fall in resistance within 18 min after starting the reaction, suggesting a steep increase in solution conductance, which is an indication of increased abundance of ions [e.g., K^+, ^{t}BuO$^-$ or **2**, and $Et_3(^t$BuO)SiH$^-$ (**2s**)] in the solution during this time. The cation−π interaction shown in **2** is likely to facilitate the dissociation of KO^{t}Bu. Dissociation simultaneously produces the ^{t}BuO$^-$ needed to form the hydride donor **2s**. Once the reaction of **2** with **2s** starts, the ion availability is expected to decrease because of the formation of neutral ion pair **3a**/**3b** and silyl ether **3s**. This behavior is consistent with the gradual increase in resistance after 18 min of the reaction (Figure 3c). This conductivity study is consistent with the observation that the reaction has an induction period before product formation commences, as detected by MS, and also provides a possible explanation for why NaO^{t}Bu does not succeed as a catalyst.[9]

NMR and EPR Studies. This reaction was also studied by NMR. We failed to observe any intermediate signals relevant to either ionic or radical mechanisms, indicating that the concentrations of intermediates were too small to be detected. We also performed EPR studies (SI, Figure S11), and we did detect a silyl radical species (*vide infra*) but not any type of indole radical intermediates. MS is a more highly sensitive technique than NMR or EPR spectroscopy, and has an established role in detecting transient ionic intermediates.[35−37]

Reactions of Different Heteroarenes. When the silylation reaction was performed in a competition experiment[9] involving different heteroarenes, such as a sulfur-containing heteroarene (thiophene), oxygen-containing heteroarene (furan), and nitrogen-containing heteroarene (1-methylpyrrole), the reactivity order was found to be thiophene > furan >1-methylpyrrole, which corresponds to the order of acidity of these heteroarenes (pK_a of C2−H proton is ~33 for thiophene, ~36 for furan, and ~40 for 1-methylpyrrole in THF).[15] These results are consistent with the deprotonation of the heteroarene being the rate-determining step of the catalytic cycle, which is also supported by DFT calculations (see later).

When the silylation reaction was carried out on electron-deficient heteroarenes such as pyridine, quinoline, isoquinoline, and acridine, no reaction or <5% product was observed.[9] This observation can also be explained by the ionic mechanism, if deprotonation is rate-limiting. First, the pK_a values for all the C−H bonds in these substrates are very high (average pK_a greater than 40 in THF) and these substrates are much less susceptible to deprotonation by the base.[15] Second, the electron-deficient nature of these heterocycles decreases the likelihood of the cation−π interaction. Third, the localized lone pair on the heterocyclic nitrogen has a tendency to complex with potassium,[38] further weakening any cation−π interactions.

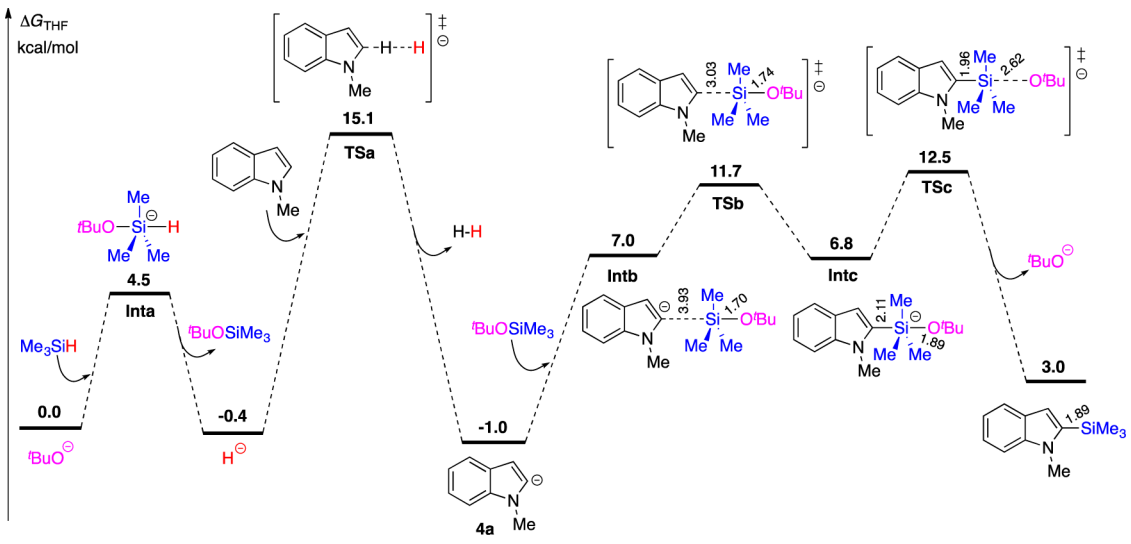

Figure 4. Free energy diagram of the ionic mechanism for KO^{t}Bu-catalyzed silylation of 1-methylindole (energy required to dissociate KO^{t}Bu into ions not included). See SI for details.

DOI: 10.1021/jacs.6b13032
J. Am. Chem. Soc. XXXX, XXX, XXX−XXX

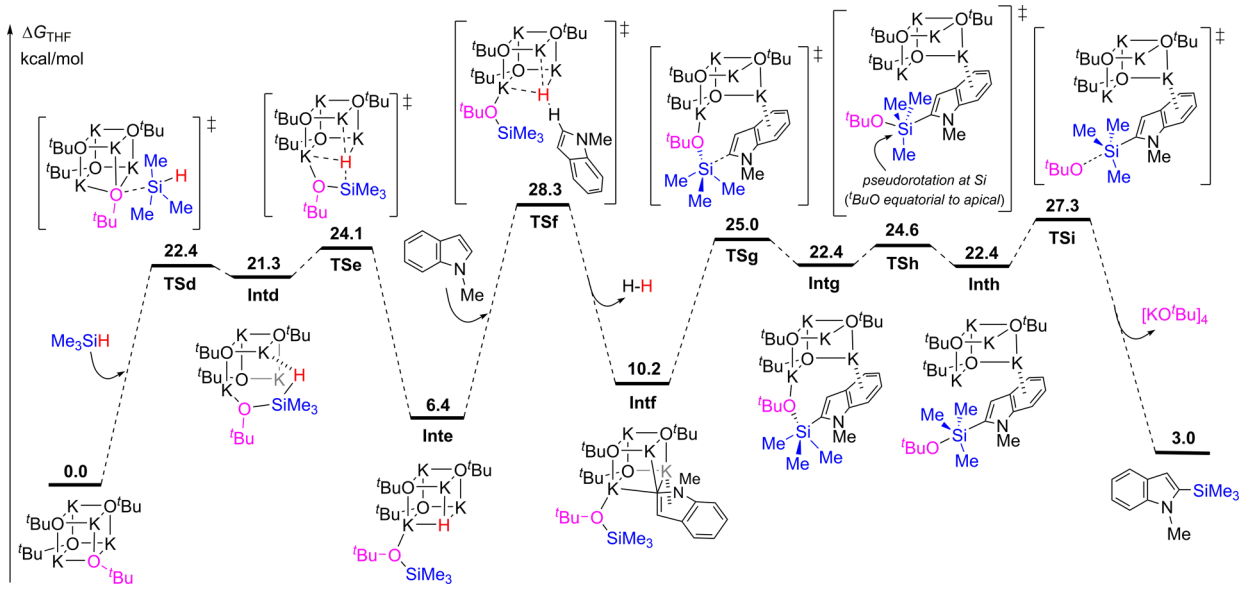

Figure 5. Free energy diagram of the neutral heterolytic mechanism for KO^{t}Bu-catalyzed silylation of 1-methylindole.

The nature of alkyl/aryl substituents in the heteroarene and silane (R^1, R^2, and R^3; Schemes 1 and 2) affect the yield in a manner consistent with the proposed catalytic cycle.[9] With increasing *+I* and/or *+R* effect[39] of the alkyl/aryl substituents attached to the heteroarene **1** (R^1 and R^2), the reaction rate and yield were lower,[9] consistent with the lower acidity of **2**. In contrast, with increasing *+I* effect of alkyl substituents (R^3) on the hydrosilane (**1s**), the reaction efficiency was found to increase,[9] consistent with more facile hydride elimination from **2s**. These substituent effects are further evidence for rate-determining deprotonation.

DFT Calculations. We computed the free energy profile of the ionic mechanism with DFT. Figure 4 summarizes the results from calculations performed with M06-2X/6-311+G-(d,p)-CPCM(THF)//B3LYP/6-31G(d) on the reaction of ^{t}BuO$^-$ with MI and a model silane, Me_3SiH, in THF. After formation of the pentacoordinate intermediate **Inta** (analogous to **2s**), dissociation of the Si−H bond gives H$^-$ and ^{t}BuOSiMe$_3$. The hydride ion then deprotonates MI, via transition state **TSa**, generating 2-indolyl anion **4a** plus H_2. The deprotonation is regioselective: C2 deprotonation is favored by 3.8 kcal/mol relative to C3 deprotonation (via **TSa_C3**, SI, Figure S8). Next, nucleophilic addition of 2-indolyl anion **4a** to ^{t}BuOSiMe$_3$ via **TSb** leads to pentacoordinate intermediate **Intc** (analogous to **5a**). Finally, dissociation of ^{t}BuO$^-$ via **TSc** gives the silylated heteroarene product.

The calculations predict that the deprotonation of the heteroarene is the rate-limiting step of the ionic mechanism, consistent with the experimental results discussed above. The computed barrier ($\Delta G^{\ddagger}$) relative to Me_3SiH, ^{t}BuO$^-$, and MI is 15.1 kcal/mol. This barrier would be easily surmountable at the temperatures typically used for the silylation reaction (25−65 °C), which suggests that the formation of the cation−π complex between MI and K$^+$ is not strictly essential for deprotonation to occur (although it would make the heteroarene more acidic). The major role of cation−π complex formation in this mechanism is to promote the dissociation of the KO^{t}Bu tetramer into K$^+$ and ^{t}BuO$^-$ ions.

A Complementary Neutral Heterolytic Mechanism. The above calculations predict that the ionic mechanism described in Scheme 2 is facile, provided that H$^-$ can be readily generated in the reaction mixture. The DESI-MS analyses (Figure 1) and conductivity experiments (Figure 3c) indicate that KO^{t}Bu dissociates, at least partially, into ions under the reaction conditions. We also considered an alternative mechanism that does not require dissociation of the tetramer (Figure 5). This mechanism is broadly analogous to the ionic pathway, but the intermediates are neutral. First, a Si−O bond is formed between Me_3SiH and the KO^{t}Bu tetramer via transition state **TSd**, giving pentacoordinate intermediate **Intd**. Next, the Si−H bond of **Intd** undergoes heterolysis (**TSe**). Rather than liberating a free H$^-$ ion, this step leads to hydride complex **Inte**, in which H$^-$ occupies one corner of the K_4X_4 unit and ^{t}BuOSiMe$_3$ is coordinated to potassium. The coordinated hydride then deprotonates MI, via **TSf**, leading to carbanion complex **Intf** and H_2. Intramolecular Si−C bond formation (**TSg**), followed by pseudorotation (**TSh**) and finally dissociation of ^{t}BuO$^-$ (**TSi**), gives the silylated heteroarene product.

Like the ionic mechanism, the rate-determining step of the neutral heterolytic (tetrameric) mechanism is the deprotonation of the heteroarene (**TSf**). The overall barrier relative to Me_3SiH, $(KO^tBu)_4$, and MI is 28.3 kcal/mol. Deprotonation of MI is regioselective; the barrier for C2 deprotonation is 5.0 kcal/mol lower than that for C3 deprotonation (see the SI). The neutral mechanism is driven by the dipolar effects mediated by the tetrameric K_4 cluster. In the initial stage of the reaction, the pentacoordinate silicon intermediate **Intd** is stabilized by interaction of the silane hydrogen with the nearby potassium ion. In carbanion complex **Intf**, and subsequent intermediates in the catalytic cycle, the heteroarene engages in a cation−π interaction with potassium. Although the computed barrier of the neutral mechanism (28.3 kcal/mol) is significantly higher than the barrier for the ionic mechanism shown in Figure 4 (15.1 kcal/mol), this does not necessarily mean that the ionic mechanism (Figure 4) is favored over the neutral mechanism (Figure 5). These barriers are calculated with respect to different sets of reactants and the calculations in Figure 4 do not include the initial dissociation of the KO^{t}Bu tetramer into ions.

DOI: 10.1021/jacs.6b13032
J. Am. Chem. Soc. XXXX, XXX, XXX−XXX

The tetrameric mechanism, with a rate-determining deprotonation step, provides alternative explanations for the important features of the silylation chemistry discussed above. First, for example, the inability of NaO^{t}Bu to catalyze the silylation can be explained by the observation that the transition state for deprotonation of MI (analogous to **TSf**) in a reaction catalyzed by NaO^{t}Bu has a barrier of 38.9 kcal/mol, more than 10 kcal/mol higher than the barrier for **TSf** in the KO^{t}Bu-catalyzed silylation. This barrier is too high for the reaction to occur under the typical experimental conditions, and reflects the weaker basicity of the more tightly bound hydride in the sodium analogue of **Inte**. Second, the computed barriers for deprotonation of other heteroarenes (thiophene, furan, and 1-methylpyrrole) with the KO^{t}Bu tetramer as the catalyst predict the correct order of reactivities measured experimentally.[9] Third, the barriers for deprotonation of electron-deficient substrates pyridine and PhCN (which failed to undergo the silylation[9]) are calculated to be 2−4 kcal/mol higher than the barrier for deprotonation of MI. Indeed, it is easier for these two electron-deficient substrates to form a C−O bond with the KO^{t}Bu tetramer[40] than to undergo deprotonation (see SI, Supplementary Note 3).

Finally, in the original 2015 paper,[9] it was reported that the reaction was inhibited by 20 mol% TEMPO. We believe that this inhibition can be readily explained as outlined in Scheme 3.

Scheme 3. Inhibition of the Silylation Reaction by TEMPO

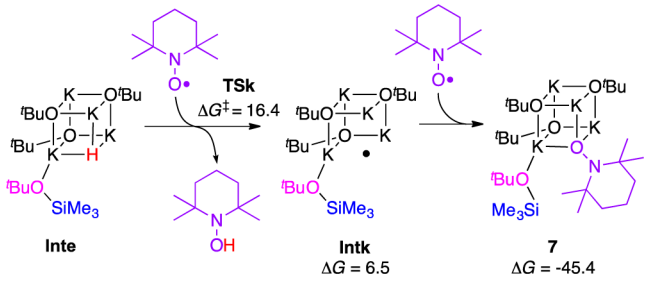

H-abstraction by TEMPO from the catalytic intermediate **Inte** has a very low activation energy (DFT calculations give a $\Delta G^{\ddagger}$ = 16.4 kcal/mol), giving **Intk** and TEMPO-H. This effectively removes **Inte** (the key base required for the deprotonation of the heteroarene) from the reaction mixture. Radical **Intk** would be expected to be trapped by TEMPO at close to diffusion-controlled rates to give a stable adduct **7**.

As **Inte** (Scheme 3) is a reasonably good H atom donor, the presence of a trace of oxygen in the reaction mixture could also promote the formation of an intermediate HO_2 complex by the donation of H atom from **Inte** to O_2 (SI, Figure S10). The resulting HO_2 complex could then undergo O−O homolysis giving OH and a coordinated oxyl radical. These radical species could presumably then abstract H from the silane to generate silyl radicals (detected in our EPR study, SI, Figure S11). The overall barrier for the formation of OH and coordinated oxyl radicals by this pathway is 24.7 kcal/mol (SI, Figure S10). Detailed studies of radical pathways for the KO^{t}Bu-catalyzed silylation reaction are presented separately in the accompanying paper.[13]

CONCLUSION

In summary, we suggest two plausible mechanisms—one ionic, the other a neutral heterolytic mechanism—for the KO^{t}Bu catalyzed C−H silylation of heteroarenes, based on a combination of empirical evidence and DFT calculations. The two mechanisms are closely related, featuring cation−π interactions, preferential abstraction of the C2-proton from the heteroarene, and formation of pentacoordinate silicon species, all of which were observed experimentally. The key steps are nucleophilic attack of KO^{t}Bu on the silane to form a reactive pentacoordinate silicon species, followed by rate-limiting Si−H heterolysis, deprotonation of the heteroarene substrate, addition of the heteroarene carbanion to the silyl ether intermediate, and eventually the release of ^{t}BuO$^-$ to give the silylated heteroarene product.

The computed activation barriers for both mechanisms (Figures 4 and 5) are consistent with the observed reaction time for silylation of MI under the conditions of the synthesis (48−61 h, 45 °C).[9] It is possible that both the ionic mechanism and the neutral heterolytic mechanism are operative along with other unknown mechanism(s). The ionic species detected by the DESI-MS and conductivity measurements are key intermediates in the ionic mechanism (Figure 4), but they are not essential in the neutral mechanism (Figure 5). Here, they could simply be "spectator" ions, formed by partial dissociation of the neutral intermediates. Dissociation of the 2-indolyl anion **4a** from **Intf** is computed to require 16.1 kcal/mol (ΔG), while the energy of dissociation of (2-indolyl)-SiMe$_3$(O^{t}Bu)$^-$ (analogous to **5a**) from **Inth** is 7.8 kcal/mol. It should be noted that the neutral intermediates involved in the neutral heterolytic mechanism (Figure 5) could also be fragmented inside the charged microdroplet resulting in gas-phase ions, which were detected in the DESI-MS experiment (Figure 1). Analyte fragmentation or transformation in charged microdroplets is known to be possible.[17,41,42] It should also be noted that the silylation reaction also proceeds with other bases (catalysts) like KOEt, KHMDS, or KOTMS,[9] which are less likely to follow the tetrameric mechanism (Figure 5), and more likely to follow the ionic mechanism similar to Scheme 2. Recently, charged microdroplets have been demonstrated to accelerate reactions.[17,43] It is therefore quite possible that some differences occur, perhaps even very important ones, in looking at the same reaction in bulk solution.[44] Nonetheless, the ionic and heterolytic mechanisms are consistent with the combined results of the DESI-MS, NMR, and conductivity experiments and can successfully explain the observed reactivities and selectivities of different heteroarenes and catalysts in the silylation process.

EXPERIMENTAL SECTION

Materials. All the necessary chemicals were purchased from Sigma-Aldrich (St. Louis, MO). The deuterated 1-methylindole (MI) was prepared according to the literature procedure.[45] HPLC grade solvents were purchased from Fisher Scientific (Nepean, ON, Canada).

Silylation reaction[9] for mass spectrometric study. In a nitrogen-filled glovebox, 0.1 mmol (~13 μL) of MI and 0.05 mmol (20 mol%, 2.5 mg) of KO^{t}Bu were added to 100 μL of dry THF taken in a 2 dram scintillation vial equipped with a magnetic stirring bar, followed by the addition of 0.3 mmol (~50 μL) of Et$_3$SiH (by filtering through a short pad of activated alumina before use). The vial was then sealed and the mixture was stirred at 30 °C. After 2 h of the reaction, a 20 μL reaction aliquot was pipetted out and dispensed immediately onto the DESI spray spot (on a glass plate, solvent = 1:1 v/v ACN and DMF) created at around 2 mm away from the heated capillary inlet of the mass spectrometer (see SI, Figure S1).

Desorption Electrospray Ionization Mass Spectrometry. The DESI-MS studies[14] were performed on a high-resolution mass spectrometer (Thermo Scientific LTQ Orbitrap XL Hybrid Ion Trap-Orbitrap mass spectrometer) using a home-built DESI source.

DOI: 10.1021/jacs.6b13032
J. Am. Chem. Soc. XXXX, XXX, XXX−XXX

The source was constructed by using an inner fused silica capillary (100 μm i.d. and 360 μm o.d.) for solvent delivery, and an outer (coaxial) stainless steel capillary (0.5 mm i.d. and 1.6 mm o.d.) for nebulizing gas (nitrogen) delivery as shown in SI, Figure S1. A stream of charged microdroplets, produced from this DESI source at ambient temperature and atmospheric pressure, was directed to the analyte surface (on a glass plate) at an incident angle ~55° with the spray tip-to-surface distance of ~5 mm, spray tip-to-mass spectrometric inlet distance of ~10 mm, and collection angle of ~5°. The charged droplets were produced either in negative ion mode (−5 kV spray voltage) or at positive ion mode (+5 kV spray voltage), at 10 μL/min solvent (1:1 v/v ACN and DMF) flow through silica tubing with the coaxial nebulizing gas flow (N_2 at 120 psi). The splashing of these charged microdroplets on the analyte surface resulted in the formation of secondary microdroplets encapsulating the analyte molecules (ions), which were then transferred to the mass spectrometer through a heated capillary causing the complete desolvation of the analyte ions. The heated capillary (MS inlet) temperature and voltage were maintained at 275 °C and 44 V, respectively. All experiments were carried out under identical conditions, unless otherwise stated. The ion optics were tuned to get maximum ion count. Data acquisition was performed for 1 min using XCalibur software (Thermo Fisher Scientific)

Electrospray Ionization Mass Spectrometry. ESI-MS studies[20,46] were performed on the same mass spectrometer as mentioned above with a home-built ESI source similar to the above DESI source. The analyte solution (in methanol) was injected to the ESI source (on-axis) at a flow rate 5 μL/min in positive ion mode (+5 kV) with a coaxial sheath gas flow (N_2 at 120 psi). The mass spectrometer inlet capillary temperature was maintained at 275 °C, and capillary voltage was kept at 44 V. The spray distance (the on-axis distance from spray tip to the entrance of the heated capillary) was kept at 1.5 cm. All experiments were carried out under identical conditions. The ion optics were tuned to get maximum ion count. Data acquisition was performed for 1 min using XCalibur software (Thermo Fisher Scientific)

Gas Chromatography. Hydrogen gas evolved from the reaction mixture was analyzed by GC on a carbon-based molecular sieve column (HP MOLSIV 30 m × 0.320 mm i.d., 12 μm) with a thermal conductivity detection (TCD). A Hewlett-Packard 5890 GC with a split−splitless injector was operated in the splitless mode for 0.5 min at which point the injector was purged with a split flow of 20 mL/min. Ultra-high-purity nitrogen was used for carrier gas, and the column was operated at a constant flow rate of 2.2 mL/min (37 cm/s average linear velocity). Oven temperature was isothermal at 32 °C. Injections of 50 μL were performed manually with a gastight syringe. The injector was maintained at 150 °C and the detector at 200 °C. Hydrogen eluted at approximately 2 min under these conditions. Absence of interference from other gases that were expected to be in any injection mixture was tested empirically.

Studying Electrolytic Properties of the Reaction by Sourcemeter. The electrolytic properties of the reaction system (mixture of 1 mmol of MI, 3 mmol of Et_3SiH, and 0.2 mmol of KO^tBu in 1 mL of anhydrous THF) and controls (anhydrous THF or 0.2 mmol of KO^tBu/sodium *tert*-butoxide in anhydrous THF or the reaction mixture without substrate) were assessed by a Keithley 2400 sourcemeter by measuring the resistance (R) of the above systems over time at 45 °C. A constant current of 0.5 μA was applied to the sourcemeter during the experiment using a four-wire setup (Cu−Sn electrodes) to measure the potential drop between the inner contacts, which was then converted to resistance value.

Computational Details. All the calculations were carried out with Gaussian 09.[47] Geometry optimizations were performed with the B3LYP method[48−51] using the 6-31G(d) basis set[52−54] for all atoms. Frequency analyses verified that the stationary points were minima or first-order saddle points. Single-point energies were calculated at the M06-2X[55]/6-311+G(d,p) level, with solvent effects (solvent = THF) modeled using the CPCM[56−58] solvation model. Gibbs free energies in THF at 298.15 K were calculated by adding the thermochemical quantities derived from the B3LYP frequencies to the M06-2X solution-phase electronic potential energy and then correcting the energy to a standard state of 1 mol/L. Computed structures are illustrated using CYLview.[59]

■ ASSOCIATED CONTENT

Supporting Information

The Supporting Information is available free of charge on the ACS Publications website at DOI: 10.1021/jacs.6b13032.

Mass spectra, NMR spectra, and DFT calculations (PDF)

■ AUTHOR INFORMATION

Corresponding Authors

*e.krenske@uq.edu.au
*houk@chem.ucla.edu
*zare@stanford.edu

ORCID

Yun-Fang Yang: 0000-0002-6287-1640
Robert H. Grubbs: 0000-0002-0057-7817
Brian M. Stoltz: 0000-0001-9837-1528
Elizabeth H. Krenske: 0000-0003-1911-0501
Kendall N. Houk: 0000-0002-8387-5261
Richard N. Zare: 0000-0001-5266-4253

Author Contributions

#S.B., Y.-F.Y., and I.D.J. contributed equally to this work.

Notes

The authors declare no competing financial interest.

■ ACKNOWLEDGMENTS

Authors thank N. Dalleska (Caltech), R. Pfattner (Stanford), and M. R. Angell (Stanford) for their help. This work was supported by the National Science Foundation under the CCI Center for Selective C−H Functionalization (CHE-1205646 and CHE-1361104), Air Force Office of Scientific Research through Basic Research Initiative grant (AFOSR FA9550-16-1-0113), and the Australian Research Council (FT120100632 to E.H.K.). Calculations were performed on the Hoffman2 cluster at UCLA and the Extreme Science and Engineering Discovery Environment (XSEDE), which is supported by the NSF, and the National Facility of the Australian National Computational Infrastructure.

■ REFERENCES

(1) Armor, J. N. *Catal. Today* **2011**, *163*, 3.
(2) Sun, C.-L.; Shi, Z.-J. *Chem. Rev.* **2014**, *114*, 9219.
(3) Yanagisawa, S.; Ueda, K.; Taniguchi, T.; Itami, K. *Org. Lett.* **2008**, *10*, 4673.
(4) Deng, G.; Ueda, K.; Yanagisawa, S.; Itami, K.; Li, C.-J. *Chem. - Eur. J.* **2009**, *15*, 333.
(5) Sun, C.-L.; Li, H.; Yu, D.-G.; Yu, M.; Zhou, X.; Lu, X.-Y.; Huang, K.; Zheng, S.-F.; Li, B.-J.; Shi, Z.-J. *Nat. Chem.* **2010**, *2*, 1044.
(6) Shirakawa, E.; Itoh, K.-i.; Higashino, T.; Hayashi, T. *J. Am. Chem. Soc.* **2010**, *132*, 15537.
(7) Rueping, M.; Leiendecker, M.; Das, A.; Poisson, T.; Bui, L. *Chem. Commun.* **2011**, *47*, 10629.
(8) Rathore, V.; Sattar, M.; Kumar, R.; Kumar, S. *J. Org. Chem.* **2016**, *81*, 9206.
(9) Toutov, A. A.; Liu, W.-B.; Betz, K. N.; Fedorov, A.; Stoltz, B. M.; Grubbs, R. H. *Nature* **2015**, *518*, 80.
(10) Uematsu, R.; Maeda, S.; Taketsugu, T. *Chem. - Asian J.* **2014**, *9*, 305.

DOI: 10.1021/jacs.6b13032
J. Am. Chem. Soc. XXXX, XXX, XXX−XXX

(11) Schneider, N.; Finger, M.; Haferkemper, C.; Bellemin-Laponnaz, S.; Hofmann, P.; Gade, L. H. *Chem. - Eur. J.* **2009**, *15*, 11515.
(12) Dubois, J.-E.; Boussu, M. *Tetrahedron Lett.* **1970**, *11*, 2523.
(13) Liu, W.-B.; Schuman, D. P.; Yang, Y.-F.; Toutov, A. A.; Liang, Y.; Klare, H. F. T.; Nesnas, N.; Osetreich, M.; Blackmond, D. G.; Virgil, S. C.; Banerjee, S.; Zare, R. N.; Grubbs, R. H.; Houk, K. N.; Stoltz, B. M. *J. Am. Chem. Soc.* **2017**, DOI: 10.1021/jacs.6b13031, (preceding paper in this issue).
(14) Takáts, Z.; Wiseman, J. M.; Gologan, B.; Cooks, R. G. *Science* **2004**, *306*, 471.
(15) Shen, K.; Fu, Y.; Li, J.-N.; Liu, L.; Guo, Q.-X. *Tetrahedron* **2007**, *63*, 1568.
(16) Wouters, J. *Protein Sci.* **1998**, *7*, 2472.
(17) Banerjee, S.; Zare, R. N. *Angew. Chem., Int. Ed.* **2015**, *54*, 14795.
(18) Lee, J. K.; Banerjee, S.; Nam, H. G.; Zare, R. N. *Q. Rev. Biophys.* **2015**, *48*, 437.
(19) Dolgov, B. N.; Kharitonov, N. P.; Voronkov, M. G. *Zh. Obshch. Khim.* **1954**, *24*, 1178.
(20) Banerjee, S.; Mazumdar, S. *Int. J. Anal. Chem.* **2012**, *2012*, 282574.
(21) Wireduaah, S.; Parker, T. M.; Lewis, M. *J. Phys. Chem. A* **2013**, *117*, 2598.
(22) Dougherty, D. A. *Acc. Chem. Res.* **2013**, *46*, 885.
(23) Kumpf, R.; Dougherty, D. *Science* **1993**, *261*, 1708.
(24) Zhu, D.; Herbert, B. E.; Schlautman, M. A.; Carraway, E. R. *J. Environ. Qual.* **2004**, *33*, 276.
(25) Lu, Q.; Oh, D. X.; Lee, Y.; Jho, Y.; Hwang, D. S.; Zeng, H. *Angew. Chem., Int. Ed.* **2013**, *52*, 3944.
(26) Steed, J. W.; Atwood, J. L. *Supramolecular Chemistry*; Wiley: Weinheim, 2013.
(27) Yang, L.; Hubbard, T. A.; Cockroft, S. L. *Chem. Commun.* **2014**, *50*, 5212.
(28) Mayr, H.; Basso, N.; Hagen, G. *J. Am. Chem. Soc.* **1992**, *114*, 3060.
(29) Larson, G. L.; Fry, J. L. *Ionic and Organometallic-Catalyzed Organosilane Reductions*; Wiley: Weinheim, 2009.
(30) Schlosser, M. *Organometallics in Synthesis, Third Manual*; Wiley: Weinheim, 2013.
(31) Blackwell, J. M.; Sonmor, E. R.; Scoccitti, T.; Piers, W. E. *Org. Lett.* **2000**, *2*, 3921.
(32) Meals, R. N. *J. Am. Chem. Soc.* **1946**, *68*, 1880.
(33) Chernyak, N.; Dudnik, A. S.; Huang, C.; Gevorgyan, V. *J. Am. Chem. Soc.* **2010**, *132*, 8270.
(34) Chisholm, M. H.; Drake, S. R.; Naiini, A. A.; Streib, W. E. *Polyhedron* **1991**, *10*, 337.
(35) Ingram, A. J.; Boeser, C. L.; Zare, R. N. *Chem. Sci.* **2016**, *7*, 39.
(36) Santos, L. S. *J. Braz. Chem. Soc.* **2011**, *22*, 1827.
(37) Eberlin, M. *Eur. Mass Spectrom.* **2017**, *13*, 19.
(38) Brown, D. J. *The Chemistry of Heterocyclic Compounds, Pyridine Metal Complexes*; Wiley: Weinheim, 2009.
(39) Smith, M. B.; March, J. *March's Advanced Organic Chemistry: Reactions, Mechanisms, and Structure*; Wiley: Weinheim, 2007.
(40) Barham, J. P.; Coulthard, G.; Emery, K. J.; Doni, E.; Cumine, F.; Nocera, G.; John, M. P.; Berlouis, L. E. A.; McGuire, T.; Tuttle, T.; Murphy, J. A. *J. Am. Chem. Soc.* **2016**, *138*, 7402.
(41) Banerjee, S.; Prakash, H.; Mazumdar, S. *J. Am. Soc. Mass Spectrom.* **2011**, *22*, 1707.
(42) Banerjee, S. *J. Mass Spectrom.* **2013**, *48*, 193.
(43) Lee, J. K.; Banerjee, S.; Nam, H. G.; Zare, R. N. *Q. Rev. Biophys.* **2015**, *48*, 437.
(44) Banerjee, S.; Gnanamani, E.; Yan, X.; Zare, R. N. *Analyst* **2017**, *142*, 1399.
(45) Lane, B. S.; Brown, M. A.; Sames, D. *J. Am. Chem. Soc.* **2005**, *127*, 8050.
(46) Fenn, J.; Mann, M.; Meng, C.; Wong, S.; Whitehouse, C. *Science* **1989**, *246*, 64.
(47) Frisch, M.; Trucks, G.; Schlegel, H.; Scuseria, G.; Robb, M.; Cheeseman, J.; Scalmani, G.; Barone, V.; Mennucci, B.; Petersson, G.; et al. *Gaussian09*; Gaussian Inc.: Wallingford, CT, 2009.
(48) Lee, C.; Yang, W.; Parr, R. G. *Phys. Rev. B: Condens. Matter Mater. Phys.* **1988**, *37*, 785.
(49) Becke, A. D. *J. Chem. Phys.* **1993**, *98*, 1372.
(50) Becke, A. D. *J. Chem. Phys.* **1993**, *98*, 5648.
(51) Stephens, P. J.; Devlin, F. J.; Cheeseman, J. R.; Frisch, M. J. *J. Phys. Chem. A* **2001**, *105*, 5356.
(52) Ditchfield, R.; Hehre, W. J.; Pople, J. A. *J. Chem. Phys.* **1971**, *54*, 724.
(53) Hehre, W. J.; Ditchfield, R.; Pople, J. A. *J. Chem. Phys.* **1972**, *56*, 2257.
(54) Hariharan, P. C.; Pople, J. A. *Theor. Chim. Acta* **1973**, *28*, 213.
(55) Zhao, Y.; Truhlar, D. G. *Theor. Chem. Acc.* **2008**, *120*, 215.
(56) Barone, V.; Cossi, M. *J. Phys. Chem. A* **1998**, *102*, 1995.
(57) Cossi, M.; Rega, N.; Scalmani, G.; Barone, V. *J. Comput. Chem.* **2003**, *24*, 669.
(58) Takano, Y.; Houk, K. N. *J. Chem. Theory Comput.* **2005**, *1*, 70.
(59) Legault, C. Y. *CYLview*; Université de Sherbrooke, 2009.

DOI: 10.1021/jacs.6b13032
J. Am. Chem. Soc. XXXX, XXX, XXX−XXX